Proceedings of the International Conference on Heat Exchanger Fouling and Cleaning - 2024 (Peer-reviewed)
April 21–26, 2024, Lisbon, Portugal; Editors: H.U. Zettler and E.M. Ishiyama

DEVELOPMENT OF NOVEL CLEANING SYSTEMS FOR IMPROVING IMMERSION CLEANING BASED ON THE HUNTING BEHAVIOUR OF THE PISTOL SHRIMP

***R. Murcek[1], M. Finster[2], A. T. Georgi[1], S. Prabhu[1], E. Fuchs[1] and M. Mauermann[1]**
[1] Fraunhofer IVV, Heidelberger Str. 20, 01189 Dresden, Germany, roman.murcek@ivv-dd.fraunhofer.de
[2] TU-Bergakademie Freiberg, Lampadiusstr. 4, 09599 Freiberg, Germany

ABSTRACT

Submersion-based cleaning methods such as ultrasound cleaning or pressure flooding are used very frequently, especially in industrial parts cleaning applications and also for heat exchangers. However, these methods have weaknesses when it comes to cleaning hard-to-reach areas such as holes and grooves. Therefore, methods are needed that improve cleaning especially in these areas. In this work, systems that imitate the hunting behaviour of the pistol shrimp were developed for this purpose. By abruptly closing its claw, the pistol shrimp creates a strong cavitation bubble with which it can scare off or stun attackers and prey. The aim was to generate high-speed water jets in a submerged state in order to imitate this cavitation effect. This was realised by using technical principles, which are also industrially applicable. For this purpose, two prototypes were developed, which generate targeted cavitation bubbles in different ways. The formation and implosion of the cavitation bubbles were visualized by high-speed imaging. In addition, experiments were carried out to determine the cleaning effect of the cavitating jets for a persistent test model soil. Finally, the results were evaluated and the two different approaches to create high-speed fluid jets with cavitation bubbles were assessed in terms of their cleaning performance.

INTRODUCTION

In addition to cleaning in place, also submersion-based cleaning methods after prior dismantling are of high importance for plate heat exchangers. Ultrasonic cleaning and pressure flooding are used here particularly frequently [1, 2]. With ultrasound, the cleaning performance, which is based on the cavitation of very small bubbles, is generally quite high. However, problems occur with complex geometries (e.g. undercuts, drill holes, etc.), since some areas are not accessible for cavitation. Also the removal of the detached soil can be an issue, because there is no flow during ultrasound cleaning [3, 4, 5]. Well-adjusted systems for pressure flooding, on the other hand, normally have an evenly distributed cleaning effect, but due to the comparatively lower mechanical forces of the flow it has limitations, especially when it comes to persistent soil layers [6]. As a consequence, novel technical concepts are required to improve the cleaning performance in submersion baths. The approach to solve this issue chosen in this paper is to find technical solutions that imitate the hunting and defensive behaviour of the pistol shrimp in order to improve cleaning in hard to clean areas and for persistent soils. This is intended to combine the advantages of ultrasonic cleaning and pressure flooding, which has not been technically possible so far.

As the name pistol shrimp (Alpheidae, also known as snapping shrimp) suggests, these small animals are capable of making very loud snapping sounds. The snapping sound is produced by the extremely fast closing of its snapping claw, which may reach half of its body size. A protruding plunger on the dactyl and a matching socket in the propus form the snapping claw. The simultaneous contraction of an opener and a closer muscle ensures that the claw is cocked before snapping. The built-up tension can be released by the contraction of a second closer muscle [7], which leads to an extremely fast closure of the claw [8]. This closure displaces the water from the claw and creates a high-speed water jet [9, 10]. The resulting water jet plays an important role in intraspecific communication [11] and is also used to stun and kill prey animals [9,12].

It was originally assumed that the snapping sound corresponds to this claw closure. However, Versluis et al [13] showed that the highspeed water jet fulfils cavitation conditions and forms a cavitation bubble. Using highspeed shadowgraphs and hydrophone measurements, it was shown that the collapse of this cavitation bubble causes the loud snapping sound. In addition, the collapse causes an intense pressure surge as well as luminescence phenomena.

Individual experimental studies have attempted to generate similar water jets artificially. Hess et al [14] used a simplified transparent claw model to investigate the flow when the claw closes. The artificial claw was enlarged based on similarity indices to enable visual accessibility. The artificial claw could be closed by a pretensioned spring

ISBN: 978-0-9984188-3-4; Published online www.heatexchanger-fouling.com

mechanism. The closing mechanism leads to the formation of a leading vortex ring. During the subsequent vortex cavitation, an axial re-entrant jet is generated in the hollow core of the cavitated vortex, which pushes the front further downstream, increasing the initial jet penetration depth. Based on this study, Koukouvinis et al [15] investigated the closing mechanism numerically. The simulation shows that the highspeed water jet leads to a vortex roll-up as a result of the shear layer. If the velocity of the claw closing is sufficient, the vortex core is depressurized and a cavitation ring is formed that moves axially with the jet. The collapse and rebound of the cavitation bubble leads to high pressure pulses.

Chaves [16] used an injector that created the highspeed water jet by the collision of two metal cylinders, referred to as projectile and piston. The projectile is accelerated by compressed air and collides with the piston that compresses water within a small cavity. Due to the high reproducibility of this process, a highspeed camera was not necessary. The process was visualized with successive cavitation bubbles through precise triggering and the temporal shift of the individual images in relation to the trigger signal. This would have made a temporal resolution of up to 1 million frames per second possible. The jet creates a cavitation bubble, as known from the pistol shrimp. Overall, the shape of the bubble looks like a candle flame. The conical shape is also reminiscent of a Mach cone. Accordingly, the jet moves faster than the bubble can displace liquid radially. Due to the significantly higher jet velocity compared to the jet of the snapping shrimp, the pressure surge caused by the collapse of the bubble could also be visualized.

Based on this preliminary work, the aim was to develop novel technical concepts that generate cavitation bubbles due to high-speed jets, which are also suitable for an industrial use. Therefore, two different approaches were developed and are presented within this paper. To analyse the quality of the cavitation bubbles produced by those two injector prototypes, shadowgraphy images were captured with a highspeed camera and cleaning tests were conducted with a test model soil on stainless steel samples.

METHODS AND MATERIALS

Highspeed water jet injector

The idea was to generate cavitation bubbles similar to those of the pistol shrimp, whereby the injectors developed for this purpose should generate the greatest possible cavitation power and at the same time the concepts should also be applicable for industrial use in terms of size, complexity and durability. Therefore, two individual injectors were examined with regard to cavitation formation and cleaning effect. Both are shown in Figure 1. The first injector (hereinafter referred to as injector I) consists of a metal syringe whose piston is driven by a linear motor (Figure 1a). The motor makes it possible to specify different water jet velocities. During injection, the pressure in the syringe is measured to determine the actual jet velocity. With this injector it was possible to generate mean jet velocities up to ~40 m/s. For each series of measurements, a volume of water of approximately 0.1 ml is injected into the tank through a 0.5 mm nozzle with a frequency of up to 1 Hz. The nozzle itself is merely an abrupt narrowing of the cross-section of the piston chamber, which results in a relatively high pressure loss. This loss is not taken into account when determining the jet velocity.

The second injector (hereinafter referred to as injector II) is based on a linear solenoid, which accelerates a piston (Figure 1b). With this piston water with a volume of approximately 0.31 ml is pushed out of a small chamber through a nozzle (diameter 0.5 mm) into the water tank and therefore created the water jet leading to cavitation. When the power from the solenoid is released, a spring pushes back the piston to its original position. The chamber in the front is then refilled through a check-valve.

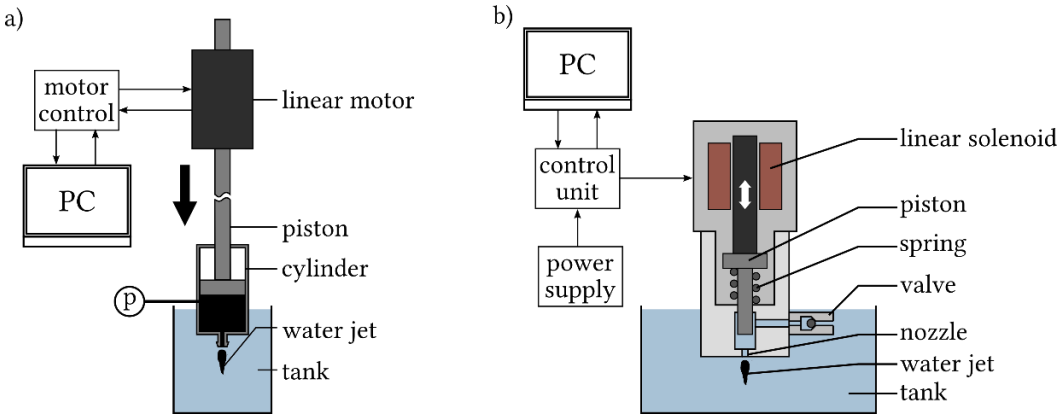

Figure 1: Different concepts for generating highspeed water jets: a) injector I, b) injector II

ISBN: 978-0-9984188-3-4; Published online www.heatexchanger-fouling.com

The maximum speed of the solenoid is determined by the electric current that is applied. The diameter ratio of the chamber and the nozzle determines the resulting pressure and therefore the jet velocity. The injector was designed to generate jet velocities that are in the range measured by Versluis et al for the pistol shrimp [13]. However, due to frictional losses on dynamic sealings it was probably slightly lower in practice. It was not possible to determine the exact values for friction and jet velocity more precisely, as it was not possible to measure the pressure in the pre-chamber for this injector. The injector was able to reliably produce constant fluid jets up to a frequency of 2.5 Hz.

Experimental setup - shadowgraphy

The cavitation bubble is observed by a shadowgraph setup as shown in Figure 2. Therefore, a highspeed water jet is injected into a tank filled with water. The light source and camera are located on opposite sides of the injector. A pair of achromatic lenses is used to collimate and refocus the light of a LED before it is received by a highspeed CMOS-camera. The LED is synchronized with the camera and stroboscopically illuminates the process with light pulses of 50 ns. The observation window is approximately 15.23 mm x 9.6 mm and has a resolution of about 12 µm per pixel. For each parameter configuration, images are captured at a frame rate of either 6200 Hz or 7500 Hz, depending on which injector is used. All experiments are performed in deionised water.

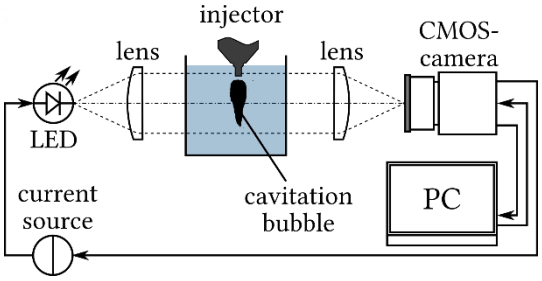

Figure 2: Schematic representation of the experimental setup for the characterization of the cavitation bubble.

The shadowgraphs are used to qualitatively assess the cavitating jet and to determine the effective range of the jet. Some image processing steps are necessary for the evaluation. All of them are performed with features of the *OpenCV* library and Python.

To obtain the mean effective length of the jet, an average image is generated from all individual raw images of a measuring series. The resulting averaged images are binarized with Otsu's method in order to obtain the relevant information. With the pixel equivalent, the pixel information could then be transferred to the physical scale.

In addition to the mean effective length of the jet, the maximum effective length was also determined from the individual images. For this purpose, the individual raw images are binarized and the maximum expansion of the jet is determined.

Experimental setup – cleaning tests

Figure 3 schematically shows the different steps of the cleaning test procedure. In the first step, a test model soil (soy yogurt) was applied reproducibly to rectangular stainless steel plates (40 mm x 20 mm). Therefore, the soil was first oversaturated onto the plates and then scraped off with a blade in a defined distance of 1 mm in order to create a uniformly thin soil layer [17]. The soiled plates were then dried for 18 h ± 1 h at 23 °C and 50 % humidity. Before the application, the soy yogurt was mixed with an optical UV tracer to make the soiled areas visible under UV light for a camera due to fluorescence [18].

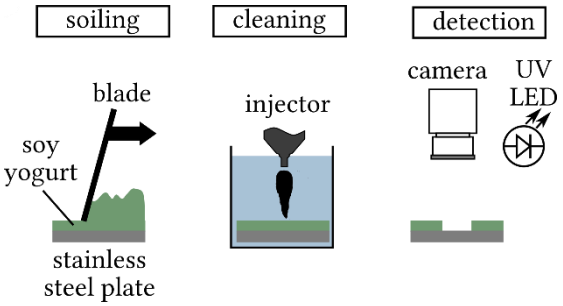

Figure 3: Schematic representation of the experimental setup for the cleaning tests

After drying, the soiled plates were put into a tank with deionised water beneath the respective injector. After a defined swelling time, several cavitating jets were shot with the injector onto the plate to remove the soil in the impact area. Table 1 shows the parameters that were varied during cleaning as well as their specific value ranges, which were selected individually for the two injectors based on preliminary tests and on the results from the shadowgraphy measurements. It was found that injector I requires longer swelling times for sufficient cleaning. For technical reasons, there were also slight differences in the nozzle distance, which could be adjusted, but this was only of minor importance when comparing the two injectors.

Table 1: Varied parameters during cleaning tests

Parameters	Injector I	Injector II
Injector distance d_I, mm	5, 10	6.5, 11, 16.5
Swelling time t_S, minutes	5, 7, 10	0.5, 2.75, 10
Number of shots n per cleaning test	3 – 20	2 – 10

ISBN: 978-0-9984188-3-4; Published online www.heatexchanger-fouling.com

After the cleaning procedure the plates were analysed with an optical sensor system based on the fluorescence of the residual soil (Figure 4).

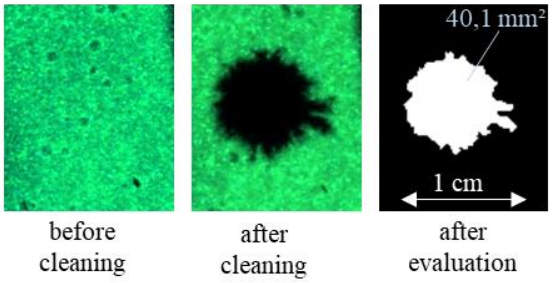

Figure 4: Exemplary images of the soiled test plates before cleaning, after cleaning and after evaluation regarding size of the cleaned area.

UV LEDs (peak at 365 nm) excite the contamination to fluorescence so that the emitted light can be detected by a camera. The fluorescence intensity is proportional to the layer thickness of the chosen soil [19]. Clean areas appear black in the captured images. In this way, the number of pixels in the cleaned area can be determined on the test plates, by setting a brightness threshold value for the clean surface. Since the size of the test plate and therefore the size of one pixel is known, also the size of the cleaned area in mm² can be calculated from this. The determined cleaned area is used to compare the different cleaning tests with regard to the influence of the operating parameters [20, 21]. Figure 4 shows exemplary images of the soiled plates after soiling, after cleaning and after the examination regarding the size of the cleaned area.

In order to be able to evaluate the cleaning results with the two injectors in terms of their industrial relevance, additional cleaning tests were carried out with soiled test plates in a conventional ultrasonic bath. The cleaning time determined there was then compared with the cleaning performance of the injectors.

RESULTS

Shadowgraphy

Figure 5 shows an example of the time course of a characteristic cavitating jet from both injectors. The black areas indicate the gas phase. It can be seen that both injectors fulfill the cavitation conditions. However, the jets are clearly different from those of a pistol shrimp. The pistol shrimp forms one big bubble, while both injectors tend to form a jet with many small bubbles, what is also called cloud cavitation. This indicates that the initial jet acceleration is significantly lower than that of the pistol shrimp. In [13] it is shown that the cavitation bubble of the pistol shrimp reaches its maximum size after approx. 0.375 ms. Both injectors require a longer time interval for this (injector I: approx. 0.8 ms, injector II: approx. 1.77 ms). The resulting lower acceleration therefore leads to the clear differences in the shape of the cavitating jet despite similar jet velocities.

In addition to the differences to the pistol shrimp, there are also major differences between the two injectors. Injector I forms a large cavitation bubble at the tip of the jet, which collapses at a distance of approx. 10 mm in front of the nozzle. The following jet only leads to local cavitation phenomena in the area close to the nozzle (about 3 mm). The entire cavitation cycle takes about 1.5 ms. The second injector generates a much larger cavitation cloud. In addition to the size of the bubble, the time scale of bubble formation also differs (about 10 ms). This is due to the larger volume of water that is injected with a single jet and the associated longer injection time. This means that the two injectors are only comparable to a limited extent.

Table 2 provides an overview of the relevant effective ranges of the jet. The mean effective length indicates the average distance from the nozzle at which cavitation occurs during jet injection. This value is based on an average image of all images in which cavitation is visible. The "maximum effective length" describes the maximum distance at which cavitation occurs. These values can be used to estimate sensible distances for the cleaning tests for both injectors. Injector I should be operated at a distance of $d_I < 10$ mm. Injector II, on the other hand, can also be used at greater distances. The observation window of the shadowgraphs is not sufficient to show the maximum effective length of the jet for this injector. However, a distance of approx. 15 mm should be feasible.

Table 2: Effective range of the cavitating jet

Parameters	Injector I	Injector II
Mean effective length, mm	< 3.1	< 11.7
Maximum effective length, mm	< 10.4	>14.7

ISBN: 978-0-9984188-3-4; Published online www.heatexchanger-fouling.com

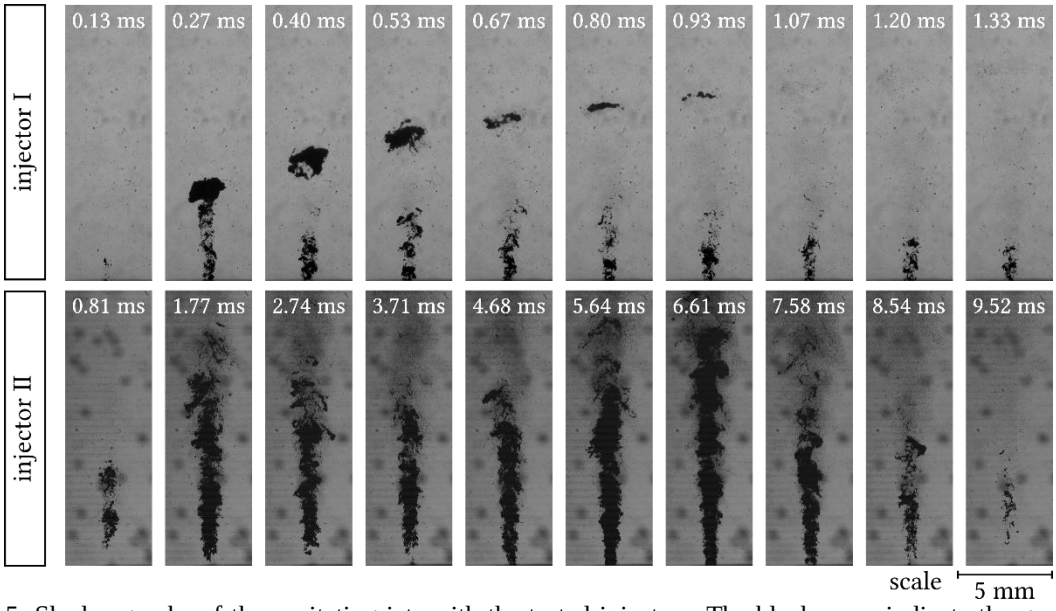

Figure 5: Shadowgraphs of the cavitating jets with the tested injectors. The black areas indicate the gas phase. The different time scales of cavitation process should be noted. The time scales in combination with the differences in the injected water volume mean that the two injectors are only comparable to a limited extent.

Cleaning tests

The cleaning tests with the injector I were conducted at distances of 5 mm and 10 mm and with swelling times of 5 min, 7 min and 10 min while the number of shots was held constant at 10. The cleaning results, which could be measured with these parameters are shown in Figure 6.

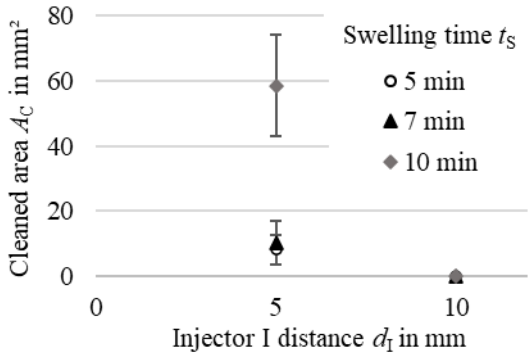

Figure 6: Cleaning results for injector I depending on the injector distance d_I and the swelling time t_S with 10 shots per cleaning test.

For distances d_I of 10 mm and higher no cleaning effect could be measured. For low distances it showed that the size of the cleaned area highly depends on the swelling time. As long as swelling has not progressed sufficiently and adhesive forces between the soil and the stainless steel plate are high, only small areas are cleaned [22, 23]. After 10 min of swelling the cleaning effect increases significantly.

At a constant swelling time t_S of 10 min and a distance d_I of 5 mm also the number of shots n was varied between 3 and 20 shots per cleaning test. The results for these tests are shown in Figure 7.

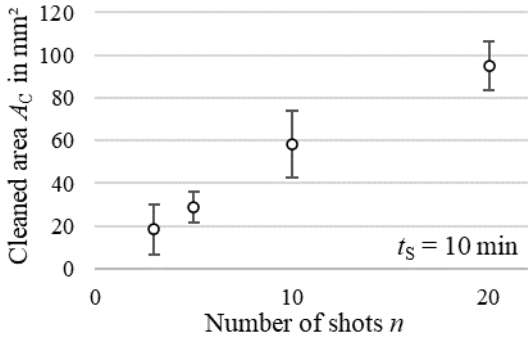

Figure 7: Cleaning results for injector I depending on the number of shots n at a constant distance d_I of 5 mm and a swelling time t_S of 10 min.

It shows that there is a linear growth in the cleaned area with an increasing shot count for the examined value range. This leads to the assumption that the intensity and the duration of the cavitating jet are not high enough to overcome adhesive and cohesive forces within the soil with a single shot and to remove it in the complete area of effect at once. Instead, only part of the soil is gradually removed from the surface with each shot.

For injector II swelling time t_S was varied in a range of 0.5 min, 2.75 min and 5 min and the distance d_I to the surface was tested at 6.5 mm, 11.5 mm and 16.5 mm. For technical reasons the distances could not be exactly the same as for injector I. The number of shots n was held constant at 10 shots each cleaning test. The influence of those parameters on the cleaned area are illustrated in Figure 8.

ISBN: 978-0-9984188-3-4; Published online www.heatexchanger-fouling.com

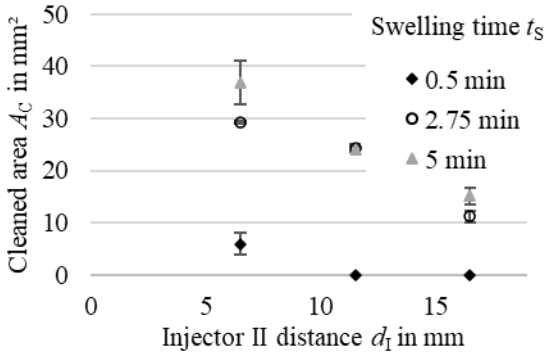

Figure 8: Cleaning results for injector II depending on the injector distance d_I and the swelling time t_S with 10 shots per cleaning test.

For the minimum swelling time of 0.5 min, which could be realised during the tests, it shows that only at a small distance of 6.5 mm a minor soil removal could be observed. For higher swelling times, on the other hand, the cleaned area was significantly increased while the difference between 2.75 min and 5 min is only marginally measurable. This shows that already after relatively short swelling times the forces of the cavitating jet are high enough to overcome the adhesion forces of the soil in the entire impact area. With increasing distance d_I, the removed soil decreases constantly but there is a significant cleaning effect measurable also at higher distances above 10 mm. For distances higher than 20 mm no significant soil removal was observable anymore.

At a constant distance d_I of 6.5 mm and swelling times t_S of 0.5 min and 2.75 min also the number of shots n with the injector was varied with regard to the influence on the cleaning effect what is shown in Figure 9. For the short swelling time of 0.5 min, no soil removal could be measured with less than 5 shots with the injector. With more than 5 shots, the cleaned area constantly increased at a very low level. For a medium swelling time of 2.75 min, a significant cleaning effect was visible already for 2 shots. During the cleaning tests with more shots, the cleaned area did not increase any further. This shows that after a sufficient reduction of the adhesive and cohesive forces within the soil layer due to swelling, the forces created by the cavitating jet of injector II are high enough to remove all soil within the whole area of effect. This is in clear contrast to injector I, where the cleaned area gradually increased the more often the surface was shot at. For the results with injector I and the swelling time t_S = 2.75 min, it must be taken into account that all experiments were conducted separately for each number of shots. The apparent drop in the cleaned area is therefore not caused by the increased number of shots, but is merely a result of the normal variation within the results of cleaning tests.

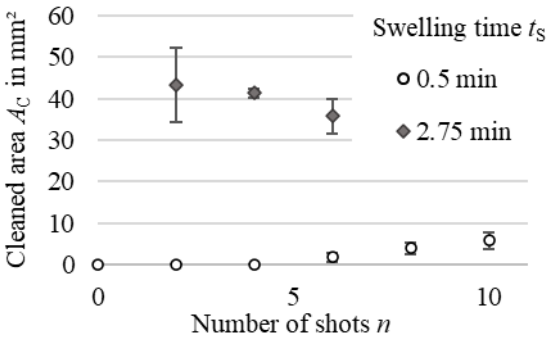

Figure 9: Cleaning results for injector II depending on the number of shots n at a constant distance d_I of 6.5 mm and swelling times t_S of 0.5 min and 2.75 min.

To further asses the two injectors in terms of their cleaning performance, the cleaned surfaces measured with both of them under similar conditions (swelling time: 5 min, distance: 5 mm with injector I and 6.5 mm with injector II, 10 shots per cleaning test) were compared. As a result, the cleaning effect with injector II (36.9 ± 4.2 mm²) is around 3.5 times higher than with injector I (8.2 ± 4.5 mm²). However, as the two injectors generate very different cavitating jets, this parameter is only of limited significance. Injector II has also a 3 times higher fluid volume, which is injected into the cleaning bath and a longer duration of the cavitating jet what might be an explanation for the higher cleaning effect.

In terms of suitability for industrial application, the cleaning effect of the injectors was also compared to a conventional ultrasonic bath working with a frequency of 37 kHz. These cleaning tests were conducted with even test plates (100 mm x 100 mm). Soy yogurt was used as test model soil with a layer thickness before drying of 1 mm. After 30 minutes of cleaning in the ultrasonic bath, the test plates were not completely clean and an average of just over 1 % residual soil mass could still be measured on the surfaces. In comparison, a theoretical cleaning time was calculated for both injectors in a scenario where they are moved over the soiled surface to clean it completely and not only punctually in a fixed position. Equation (1) shows how this theoretical cleaning time $t_{C,th}$ is calculated taking into account fixed operating parameters, at which the best cleaning performance was achieved with each injector.

$$t_{C,th} = t_s + \frac{A_P}{A_C} * \frac{n}{f} \quad (1)$$

In this equation t_S is the swelling time, which had the best results for each injector, n is the optimum number of shots at this swelling time, f is the shot frequency, A_C is the cleaned area at these operating parameters for the minimum injector distance and A_P is the area size of the plate, for which

ISBN: 978-0-9984188-3-4; Published online www.heatexchanger-fouling.com

the theoretical cleaning time $t_{C,th}$ is calculated. The shot frequency f was 1 Hz for all cleaning tests. This calculation is an estimation and does not consider overlapping of cleaned areas and movement time of the injectors. The theoretical cleaning time $t_{C,th}$ was calculated for the small test plates as well as for the larger ones. The results of this calculation are shown in Table 3.

Table 3: Comparison of cleaning performance in ultrasonic bath to theoretical cleaning time of injectors at optimum operating parameters for two different plate sizes

Parameters	Injector I	Injector II
Injector distance d_I, mm	5	6.
Swelling time $t_{S,}$ minutes	10	2.75
Number of shots n	10	2
Cleaned area A_C, mm²	58.5 ± 15.7	43.3 ± 8.9
$t_{C,th}$ for plates 40 x 20 mm², minutes	12.3 ± 3.3	3.4 ± 0.7
$t_{C,th}$ for plates 100 x 100 mm², minutes	38.5 ± 10.3	10.4 ± 2.1
Cleaning time ultrasonic bath, minutes	> 30 minutes	

It shows that injector II is able to clean the plates significantly faster than injector I since it requires only two shots at each position after a generally shorter time of swelling. For smaller test plates, both injectors have advantages over cleaning with the ultrasonic bath. For the larger test plates, only injector II was faster than this conventional cleaning method.

CONCLUSION

Both injectors are capable of generating fluid jets with high velocities that lead to strong local cavitation in submersion-based cleaning baths. However, the shape and characteristics of the resulting cavitation differ from their original model, the pistol shrimp. While the shrimp forms one big bubble, both injectors produce cloud cavitation with many small bubbles. Furthermore, the jet shapes also differ between the two injectors. Injector I releases a smaller fluid volume within very short time and forms one large spherical bubble at the jet front. Injector II discharges a higher fluid volume into the cleaning bath and therefore produces a significantly bigger and longer cloud jet.

As a result, the forces generated on the soiled surface with injector I are smaller, so that it takes more shots and swelling time to remove the soil and it works only for distances below 1 cm. On the other hand, the maximum cleaned area is higher as for injector II since the large cavitation bubble in the jet front produces a wide area of effect on the soiled surface. Injector II in return can also be used for cleaning at distances above 1 cm. The forces on the soiled surface and the duration of the cavitating jet are higher so that already few shots can be sufficient at short swelling times to remove the soil in the complete area of effect. Since it also works at higher frequencies injector I can be considered as more time efficient. On the other hand, it requires more effort to produce the cavitating jet and to release the higher fluid volume.

At similar operating parameters, injector II removes more soil from the surface but also works with a higher discharged fluid volume and a longer jet duration. Compared to a conventional ultrasonic bath, both injectors may have advantages depending on the size of the surface to be cleaned. However, this must be investigated in further comparative tests.

The studies showed that both injectors are able to remove a persistent food model soil and to increase cleaning performance on plane surfaces by using targeted cavitation. Further tests have to be conducted to determine the cleaning effect on surfaces with complex geometries as well as to test the possibility of cleaning with a moving nozzle. Also, the suitability for other persistent soil types need to be examined further.

ACKNOWLEDGMENTS

The IGF project (22294 BR) is supported by the Research Association of the Industrial Association for Food Technology and Packaging (IVLV e.V.) and is funded by the Federal Ministry for Economic Affairs and Climate Action via the AiF as part of the program for the promotion of industrial community research (IGF) based on a decision of the German Bundestag.

NOMENCLATURE

A_C Cleaned area, mm²
A_P Plate size, mm²
d_I Injector distance
f shot frequency, s^{-1}
n number of injector shots, dimensionless
t_S Swelling time, min
t_C Cleaning time, min

Subscript
th theoretical

REFERENCES

[1] Quartly-Watson, T., *The importance of power ultrasound in cleaning and disinfection in the poultry industry - a case study*, Ultrasound in Food Processing, pp. 144–150, 1998.
[2] Bilz, M., Motschmann, S., and Mankiewicz, J., *Markt- und Trendanalyse in der Industriellen Teilereinigung 2012*, Fraunhofer-Allianz Reinigungstechnik, Berlin, 2013.

ISBN: 978-0-9984188-3-4; Published online www.heatexchanger-fouling.com

[3] Seifert, V., Mauermann, M., and Boye, A. *Component alignment and movement in the ultrasonic bath.* Journal für Oberflächentchnik 57, pp. 26–27, 2017.

[4] Hauptmann, M., Struyf, H., De Gendt, S., Glorieux, C., Brems, S., *Importance of Bubble Size Control in Ultrasonic Surface Cleaning by Pulsed High-Frequency Sound Fields,* ECS Journal of Solid State Science and Technology, Vol. 3, No. 1, pp. N3032–N3040, 2013.

[5] Kahlen, I., *Untersuchung des Reinigungseffektes von Ultraschall auf Oberflächen von Chirurgie-Instrumenten und dessen prototypische Umsetzung in ein Dekon-taminationsverfahren*, Ph.D. thesis, Technical University Berlin, 2012.

[6] Haase, B, *Bauteilreinigung – Alternativen zum Einsatz von Halogenkohlenwasserstoffen*, Expert Verlag, 1996.

[7] Ritzmann, R. E, *Mechanisms for the Snapping Behavior of Two Alpheid Shrimp, Alpheus californiensis and Alpheus heterochelis*, Journal of Comparative Physiology 95, pp. 217-236, 1974.

[8] Schmitz, B., and Herberholz, J., *The visible water jet: flow visualisation in snapping shrimp (Alpheus heterochaelis)*, Proceedings of the 26th Göttingen Neurobiology Conference, p. 241, 1998.

[9] Herberholz, J., and Schmitz, B., *Flow visualisation and high speed video analysis of water jets in the snapping shrimp (Alpheus heterochaelis)*, Journal of Comparative Physiology 185, pp. 41-49, 1999.

[10] Schein, H., *Aspects of the Aggressive and Sexual Behaviour of Alpheus heterochaelis Say*, Marine Behaviour and Physiology 3, pp. 83-96, 1975.

[11] Herberholz, J., and Schmitz, B., *Role of Mechanosensory Stimuli in Intraspecific Agonistic Encounters of the Snapping Shrimp (Alpheus heterochaelis)*, Biology Bulletin 195, pp.156-167, 1998.

[12] MacCinitie, G. E., and MacGinitie, N., *Natural History of Marine Animals*, McCraw-Hill, New York, 1949.

[13] Versluis, M., Schmit, B., von der Heydt, A., and Lohse, D., *How Snapping Shrimp Snap: Through Cavitating Bubbles*, Science 289, pp. 2114-2117, 2000.

[14] Hess, D., Brücker, C., Hegner, F., Balmert, A., and Bleckmann, H., *Vortex Formation with a Snapping Shrimp Claw*, PLOS ONE 8 no. 11, 1998.

[15] Koukouvinis, P., Brücker, C., and Gavises, M., *Unveiling the physical mechanism behind pistol shrimp cavitation*, Nature Scientific Reports 7: 13994, 2017.

[16] Chaves, H.: *Cavitation and Bubble Collapse Produced by Fast Liquid Jets (Model experiment of the snapping shrimp)*, Proceedings of the 19th International Symposium on the Application of Laser and Imaging Techniques to Fluid Mechanics, 2018.

[17] Beckmann, S., Fuchs, E., Jacob, S., Mauermann, M., *Influence of steam-induced wetting of food- and cosmetic-based contaminants on the efficiency of clean-in-place processes of containers*, Food and Bioproducts Processing, Vol. 138, pp. 14-22, 2023.

[18] Hanisch, T., Joppa, M., Eisenrauch, V., Jacob, S., and Mauermann, M., *Simulation-based optimization and experimental analysis of the cleanability of macro-structured, 3D-printed pipe surfaces with protrusions*, Food and Bioproducts Processing, Vol. 136, pp. 106-122, 2022.

[19] Mauermann, M., Majschak, J.-P., Bley, T., Bellmann, C., Calvimontes, A., and Caspari, A., *Cleanability of food contact surfaces*, Chemie Ingenieur Technik, Vol. 84, Is. 9, pp. 1568-1574, 2012.

[20] Murcek, R., Hölzel, J., Köhler, H., Boye, A., Hesse, M., and Mauermann, M., *Development of a quartz crystal sensor system to monitor local soil removal during cleaning in closed food processing lines*, Food and Bioproducts Processing, Vol. 127, pp. 282-287, 2021.

[21] Köhler, H., Stoye, H., Weyrauch, T., Boye, B., Mauermann, M., and Majschak, J.-P., *Study on the application of cleaning models with high speed water jets to CIP-Processes*, Tehnicki Vjesnik, Vol. 23, Is. 2, pp. 349 – 355, 2016.

[22] Tuladhar, T.R., Paterson, W.R., and Wilson, D.I., *Investigation of alkaline cleaning-in-place of whey protein deposits using dynamic gauging*, Food and Bioproducts Processing, Vol. 80, Is. 3, pp. 199-214, 2022.

[23] Mervade-Prieto, R., Paterson, W.R., Chen, X.D., and Wilson, D.I., *Diffusion of NaOH into a protein gel*, Chemical Engineering Science, Vol. 63, Is. 10, pp. 2763-2772 2008.

ISBN: 978-0-9984188-3-4; Published online www.heatexchanger-fouling.com